

Influence of twophoton absorption on thirddorder nonlinear optical processes as studied by degenerate fourwave mixing: The study of soluble didecyloxy substituted polyphenyls

Mingtang Zhao, Yiping Cui, Marek Samoc, Paras N. Prasad, Marilyn R. Unroe, and Bruce A. Reinhardt

Citation: *The Journal of Chemical Physics* **95**, 3991 (1991); doi: 10.1063/1.460806

View online: <http://dx.doi.org/10.1063/1.460806>

View Table of Contents: <http://scitation.aip.org/content/aip/journal/jcp/95/6?ver=pdfcov>

Published by the [AIP Publishing](#)

Articles you may be interested in

[Degenerate Four wave Mixing Studies and Ultrafast Optical Kerr Effect Measurements of Thirdorder Nonlinear Optical Response in a Charge Transfer Organic Material](#)

AIP Conf. Proc. **1391**, 689 (2011); 10.1063/1.3643650

[Twophoton absorption and second hyperpolarizability measurements in diphenylbutadiene by degenerate fourwave mixing](#)

J. Chem. Phys. **98**, 2593 (1993); 10.1063/1.464141

[Thirdorder nonlinearity and twophotoninduced molecular dynamics: Femtosecond timeresolved transient absorption, Kerr gate, and degenerate fourwave mixing studies in poly \(pphenylene vinylene\)/solgel silica film](#)

J. Chem. Phys. **94**, 5282 (1991); 10.1063/1.460512

[Photoinduced processes and resonant thirddorder nonlinearity in poly \(3dodecylthiophene\) studied by femtosecond time resolved degenerate four wave mixing](#)

J. Chem. Phys. **93**, 2201 (1990); 10.1063/1.459052

[Dynamics of resonant thirddorder optical nonlinearity in perylene tetracarboxylic dianhydride studied by monitoring first and secondorder diffractions in subpicosecond degenerate fourwave mixing](#)

J. Chem. Phys. **91**, 6643 (1989); 10.1063/1.457382



Influence of two-photon absorption on third-order nonlinear optical processes as studied by degenerate four-wave mixing: The study of soluble didecyloxy substituted polyphenyls

Mingtang Zhao, Yiping Cui, Marek Samoc, and Paras N. Prasad^{a)}

Photonics Research Laboratory, Department of Chemistry, State University of New York at Buffalo, Buffalo, New York 14214

Marilyn R. Unroe and Bruce A. Reinhardt

Nonmetallic Materials Division, Polymer Branch of Air Force Materials Laboratory, Wright-Patterson Air Force Base, Ohio 45433-6533

(Received 27 August 1990; accepted 12 June 1991)

We have investigated the influence of two-photon absorption on the third-order nonlinear optical properties of model organic molecules using the technique of degenerate four-wave mixing (DFWM). A theoretical formulation developed here shows that the presence of two-photon absorption, which is related to the imaginary part of the third-order susceptibility $\chi^{(3)}$, leads to an enhancement of the effective third-order nonlinearity and to the appearance of effects caused by the formation of two-photon generated excited states. The dynamic behavior of the nonlinearity is then governed by the properties of excited molecules. The nonlinear effects also involve contributions which depend on the fifth power of the electric field. We have performed a systematic study of third-order nonlinear optical properties of alkoxy ($-\text{C}_{10}\text{H}_{21}\text{OCH}$) substituted *p*-polyphenyl oligomers using the technique of time-resolved degenerate four-wave mixing with subpicosecond pulses at 602 nm. Experimentally determined values of the second-order hyperpolarizability γ for the oligomers increase smoothly from the monomer to the trimer, with a more rapid increase to the pentamer and to the heptamer. In addition, the hyperpolarizabilities for the pentamer and the heptamer appear to be complex. A smooth increase of the γ value is expected from an increase of the π conjugation from a shorter chain oligomer to a longer chain oligomer. The more rapid increase of the γ value in the pentamer, and especially in the heptamer, however, cannot be explained satisfactorily by only taking into account the π -conjugation length. Two-photon absorption for the pentamer and the heptamer at the measurement wavelength of 602 nm is suggested to be important as the observed dynamic behavior is satisfactorily explained by the predictions of the theoretical model presented here. It is shown that the effective γ value for a two-photon absorbing material is a function of optical intensity, pulse width, and sample length if one uses the conventional degenerate four-wave mixing description.

I. INTRODUCTION

Nonlinear optical processes in organic materials have been a subject of intense experimental and theoretical investigation during the last decade. Considerable work has been done toward understanding the microscopic origin of nonlinear behavior of organics.¹⁻⁵ Among the problems which have been addressed are those of the structure-property relationships for various possible designs of optically nonlinear molecules that can be used as building blocks for photonic materials. Here, we investigate the role of two-photon absorption which is an important factor in the performance of materials for third-order nonlinear optics. Among the various processes that are due to the presence of a third-order material nonlinearity [usually represented by the susceptibility $\chi^{(3)}(-\omega_4; \omega_1, \omega_2, \omega_3)$], the most interesting ones from a practical point of view are those which allow one to control a light beam by another light beam. In the degenerate case, this means that the propagation of a beam of frequency ω can be controlled by another beam of the same frequency; the proper susceptibility for this effect is $\chi^{(3)}(-\omega; \omega, -\omega, \omega)$. Some examples of various manifestations of this susceptibil-

ity are power-dependent refractive index,^{6,7} self-focusing,⁸⁻¹² optical Kerr effect,^{13,14} and phase conjugate reflection.¹⁵⁻¹⁹ Examination of dispersion relations derived for the third-order hyperpolarizability from quantum chemical considerations tells us that the hyperpolarizability (and third-order susceptibility) for a degenerate process will become one-photon resonant when the frequency of the light approaches a material excitation frequency. However, for $\chi^{(3)}(-\omega; \omega, -\omega, \omega)$, one can also expect resonances at combinations of input frequencies, which means that, in general, both low frequency material modes (molecular oscillations and vibrations, for example) and the modes at frequency close to 2ω will contribute to the nonlinear response. Therefore, even though a specific wavelength of light may be far from any one-photon resonance, in some materials a two-photon resonance of this frequency may dominate the nonlinearity. The role of such a resonance is dual. The values of $\chi^{(3)}$ and the corresponding microscopic coefficient γ can be enhanced considerably. However, the closeness of a resonance (one photon or two photon) also leads to the appearance of an imaginary part of the susceptibility, i.e., both γ and $\chi^{(3)}$ become complex. Furthermore, as the imaginary

^{a)} Author to whom correspondence should be addressed.

part of the first-order susceptibility is responsible for one-photon absorption and is related to the linear absorption coefficient, similarly the imaginary part of $\chi^{(3)}$ is related to two-photon absorption. Therefore, the effective nonlinearity observed in a degenerate four-wave mixing experiment may involve additional contribution due to the formation of excited species by a two-photon absorption.

The previous studies of thiophene oligomers²⁰ and poly-*p*-phenyls²¹ have indicated that molecules possessing extensively conjugated π -electron systems exhibit large optical nonlinearity. However, while an extension of the π -electron system invariably leads to a higher value of the third-order hyperpolarizability γ , there are several complicating factors which play important roles in determining the nonlinear optical response of the material. First, simple addition of more π -conjugated units to an oligomeric chain does not always bring about the desired effect of a substantial increase in γ . Due to nonplanarity of long molecules, such as oligomers of benzene, the initial rapid increase of γ accompanying an increase in the length of the molecule may saturate for longer chains.^{20,21} For the materials used for experimental investigation reported in this paper, the didicyloxy substitution renders increased solubility to the polyphenyls, so that even the pentamer and the heptamer are soluble in common organic solvents such as tetrahydrofuran. This increased solubility has permitted us to investigate the nonlinear optical response of these higher oligomers. The nonlinear optical behavior of these higher oligomers demonstrates that with the increase of conjugation length, another complicating factor to consider is two-photon absorption.

In this paper, we first present a theoretical description of degenerate four-wave mixing (DFWM) in the presence of two-photon absorption. The DFWM signal is shown to be derived from two dynamic processes. One is the coherent instantaneous four-wave mixing and the other is the Bragg diffraction from a two-photon-induced population grating. Recently, Cao²² *et al.* have also developed a theoretical formalism of transient four-wave mixing which considers both the fast (instantaneous) and slow components of the four-wave mixing signal. The experimental DFWM studies of the didicyloxy substituted poly-*p*-phenyl oligomers are conducted using the backward wave geometry. The experimental results for the pentamer and the heptamer are analyzed using the proposed theoretical description which involves two-photon processes.

II. THEORY

In general, a four-wave mixing experiment may be considered as an interaction of three optical fields in a medium. The presence of a third-order nonlinear optical susceptibility $\chi^{(3)}$ leads to the creation of various components of material polarization, which give rise to new optical fields. In favorable conditions, especially if the phase-matching condition is fulfilled (i.e., the phase relation between the waves emitted by various parts of the whole nonlinear medium leads to constructive buildup of the resulting wave), new beams of light are created. In the degenerate case, the three fields superimposed on the medium are of the same frequency and the new wave created by their interaction is also of the same

frequency. Therefore, the nonlinear susceptibility involved is $\chi^{(3)}(-\omega; \omega, -\omega, \omega)$ and the phase matching condition is $\Sigma k_i = 0$. In the phase-conjugate geometry (also called backward four-wave mixing), two beams (labeled 1 and 2) counterpropagate and a third one (3) is incident at a small angle to beam 1 (Fig. 1). The phase matching condition predicts a generation of the output beam (4), which is counterpropagating with respect to beam 3. Another way of looking at a DFWM experiment is to treat it as the creation of transient gratings by interference of pairs of waves and Bragg diffraction of the remaining wave from the grating formed in the material by its nonlinear response to spatially modulated light intensity.^{23,24} In the phase conjugation geometry, the signal beam can also be considered to be the Bragg diffraction of beam 2 from the grating formed by 1 and 3, and the Bragg diffraction of beam 1 from the grating formed by 2 and 3.

We assume for simplicity that the molecules of a two-photon absorbing medium can be treated as two-level systems and their excited state lifetime is T_1 . The third-order polarization in the material can be assumed to consist of an instantaneous part due to the coherent third-order nonlinearity (instantaneous four-photon parametric mixing) and a slow part which is due to the change of susceptibility brought about by the presence of population grating of excited states.²⁵ Thus the polarization can be expressed as

$$\mathbf{P} = \chi_a^{(1)} \cdot \mathbf{E} + \chi^{(3)} : \mathbf{E} \mathbf{E} \mathbf{E} + \frac{N_b}{N} (\chi_b^{(1)} - \chi_a^{(1)}) \cdot \mathbf{E}, \quad (1)$$

where $\chi^{(1)}$ and $\chi^{(3)}$ are the linear susceptibility and the third-order susceptibility, respectively; the indices a and b refer to the ground and the excited states, respectively. N is the total density of molecules ($N = N_a + N_b$). $\chi_b^{(1)}$ is the linear susceptibility of a hypothetical material built of excited state molecules. Therefore, the first term on the right-hand side of Eq. (1) is the linear polarization, the second term is the instantaneous third-order polarization, and the last term is the polarization increment brought about by the existence of excited species. Equation (1) refers to the relation between the vector \mathbf{P} and the vector \mathbf{E} . The susceptibilities $\chi_a^{(1)}$ and $\chi_b^{(1)}$ are tensors of the second rank, while $\chi^{(3)}$ is the tensor of the fourth rank. In the following, we replace the vectors and tensors with their scalar values. It must be kept in mind that because our experiments are carried out in liquid form, the first- and third-order susceptibilities are orientationally averaged.

The excited state density N_b is governed by the following kinetic equation:

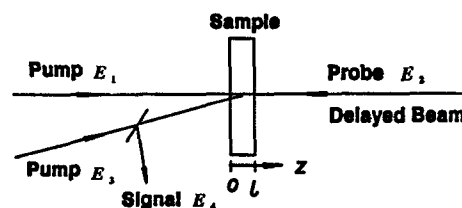


FIG. 1. The backward DFWM geometry. E_1 and E_3 are pump beams and E_2 is the probe beam in our measurement.

$$\frac{dN_b(\mathbf{r},t)}{dt} = \kappa_2 N I^2(\mathbf{r},t) - \frac{N_b(\mathbf{r},t)}{T_1} \quad (2)$$

In the above equation, T_1 is the molecular excited state lifetime, κ_2 is the two-photon absorption cross section of the molecule, and $I(\mathbf{r},t)$ is the light intensity in the medium. We ignore the influence of molecular diffusion on the decay of the population grating. Equation (2) can be solved as

$$N_b(\mathbf{r},t) = e^{-t/T_1} \int_{-\infty}^t \kappa_2 N I^2(\mathbf{r},t') e^{t'/T_1} dt' \quad (3)$$

The fields of the three incident beams (E_1 , E_2 , and E_3) and signal beam (E_4) can be expressed in the following complex scalar forms:

$$E_j(\mathbf{r},t) = \mathcal{E}_j(\mathbf{r},t) \exp[i(\mathbf{k}_j \cdot \mathbf{r} - \omega t)] \quad (j = 1,2,3,4), \quad (4)$$

where $\mathcal{E}_j(\mathbf{r},t)$ is the envelope function for the j th optical field. In the following calculation, we only consider the case in which the intensity of beam 2 (I_2) is much weaker than that of either beam 1 (I_1) or beam 3 (I_3), and in which the intensity of the signal beam (I_4) is also much weaker than that of any incident beam. Therefore, the excited state population induced by beam 2 and signal beam 4 can be neglected. In order to simplify the theoretical calculation, we only consider a case where beam 2 is polarized orthogonally to both beams 1 and 3. In this case, only the interference between E_1 and E_3 is important. The total field due to these two strong beams is given by

$$E(\mathbf{r},t) \cong E_1(\mathbf{r},t) + E_3(\mathbf{r},t) \quad (5)$$

and the intensity profile of incident beams is

$$I(\mathbf{r},t) = B \cdot E(\mathbf{r},t) \cdot E^*(\mathbf{r},t) \cong B |\mathcal{E}_1(\mathbf{r},t)|^2 + B |\mathcal{E}_3(\mathbf{r},t)|^2 + [B \mathcal{E}_1(\mathbf{r},t) \mathcal{E}_3^*(\mathbf{r},t) e^{-i(\mathbf{k}_3 - \mathbf{k}_1) \cdot \mathbf{r}} + \text{c.c.}], \quad (6)$$

where $B = nc/2\pi$ and n is the refractive index for the medium at frequency ω . From Eq. (6), we have

$$I^2(\mathbf{r},t) = B^2 [|\mathcal{E}_1(\mathbf{r},t)|^4 + |\mathcal{E}_3(\mathbf{r},t)|^4 + 4|\mathcal{E}_1(\mathbf{r},t)|^2 \cdot |\mathcal{E}_3(\mathbf{r},t)|^2] + 2B^2 \{ [|\mathcal{E}_1(\mathbf{r},t)|^2 + |\mathcal{E}_3(\mathbf{r},t)|^2] \times \mathcal{E}_1(\mathbf{r},t) \mathcal{E}_3^*(\mathbf{r},t) e^{-i(\mathbf{k}_3 - \mathbf{k}_1) \cdot \mathbf{r}} + \text{c.c.} \} + B^2 \{ \mathcal{E}_1^2(\mathbf{r},t) \mathcal{E}_3^{*2}(\mathbf{r},t) e^{-2i(\mathbf{k}_3 - \mathbf{k}_1) \cdot \mathbf{r}} + \text{c.c.} \}. \quad (7)$$

Interference terms are contained in the first and the second curly brackets. The spatial distribution of two-photon-induced species will contain the same Fourier components as those appearing in the above equation. The bias term (space-independent term) is not important for the generation of the DFWM signal. The term in the third curly bracket will only contribute to the second-order diffraction from the population grating.²⁶ Since the second-order diffraction is not phase matched under our experimental conditions, it would only be important for samples thinner than the coherence length, but not for the thick samples used in our present study. The term in the first curly bracket in the above equation will, however, contribute to DFWM in the direction of the usual phase conjugate signal. Therefore, to derive the properties of the phase conjugate beam, it suffices to consider only the proper component of the second term. Combining Eqs. (1), (3), and (7), the polarization which corresponds to the phase conjugate signal can be written as

$$P^{(3)}(z,t) = 2\chi^{(3)} \mathcal{E}_1(z,t) \mathcal{E}_2(z,t) \mathcal{E}_3^*(z,t) \exp\{i[(\mathbf{k}_1 + \mathbf{k}_2 - \mathbf{k}_3) \cdot \mathbf{z} - \omega t]\} + 2\kappa_2 B^2 (\chi_b^{(1)} - \chi_a^{(1)}) \times e^{-t/T_1} \exp\{i[(\mathbf{k}_1 + \mathbf{k}_2 - \mathbf{k}_3) \cdot \mathbf{z} - \omega t]\} \int_{-\infty}^t [|\mathcal{E}_1(z,t')|^2 + |\mathcal{E}_3(z,t')|^2] \times \mathcal{E}_1(z,t') \mathcal{E}_3^*(z,t') e^{t'/T_1} dt' \mathcal{E}_2(z,t). \quad (8)$$

The factor 2 in the first term of the above equation is a degeneracy factor. In Eq. (8), the first term describes the contribution of the coherent DFWM process and the second term describes the contribution of the population grating process. We now introduce an equivalent third-order susceptibility $\chi_g^{(3)} = \kappa_2 B^2 (\chi_b^{(1)} - \chi_a^{(1)}) T_1$, which contains a contribution from the population grating process under a cw condition or under such a condition that incident laser pulse width is much longer than the excited state decay time T_1 . We assume that the beams take the following forms:

$$\mathcal{E}_j(z,t) = E_{j0} \mathcal{F}(t - z/\vartheta_g, \tau), \quad j = 1,3, \quad (9)$$

$$\mathcal{E}_j(z,t) = E_{j0} \mathcal{F}(t + z/\vartheta_g, \tau), \quad j = 2, \quad (10)$$

where ϑ_g is the group velocity of the laser pulse in the medium, τ is the pulse width, and $\mathcal{F}(\xi, \tau)$ ($\xi = t - z/\vartheta_g$ or $t + z/\vartheta_g$) is the propagation function of the laser pulse envelope. A Gaussian or a sech² functional form may be assumed for the incident beams. The constant E_{j0} is the peak amplitude of the j th pulse. Substituting Eqs. (8)–(10) into a non-stationary coupling wave equation²⁷ and neglecting the attenuation of the optical fields, one obtains

lope. A Gaussian or a sech² functional form may be assumed for the incident beams. The constant E_{j0} is the peak amplitude of the j th pulse. Substituting Eqs. (8)–(10) into a non-stationary coupling wave equation²⁷ and neglecting the attenuation of the optical fields, one obtains

$$\frac{\partial \mathcal{E}_4(z,t)}{\partial z} - \frac{1}{\vartheta_g} \frac{\partial \mathcal{E}_4(z,t)}{\partial t} = -i \frac{2\pi\omega^2}{kc^2} P^{(3)}(z,t) e^{i(\mathbf{k}_4 \cdot \mathbf{z} + \omega t)}. \quad (11)$$

In order to solve the above differential equation, the variables z and t are replaced with z and $\eta = t + z/\vartheta_g$. If beam 2 is delayed with respect to beams 1 and 3 by T_d , Eq. (11) becomes

$$\frac{\partial \mathcal{E}_4(z,\eta)}{\partial z} = -i \frac{2\pi\omega^2}{kc^2} P^{(3)}(z,\eta, T_d) e^{i(\mathbf{k}_4 \cdot \mathbf{z} + \omega t)}, \quad (12)$$

where

$$\begin{aligned}
P^{(3)}(z, \eta, T_d) &= 2\chi^{(3)} E_{10} E_{20} E_{30}^* \mathcal{F}(\eta - T_d, \tau) \mathcal{F}^2(\eta - 2z/\vartheta_g, \tau) \exp\{i[(\mathbf{k}_1 + \mathbf{k}_2 - \mathbf{k}_3) \cdot \mathbf{z} - \omega t]\} \\
&\quad + 2\chi_g^{(3)} E_{10} E_{20} E_{30}^* \mathcal{F}(\eta - T_d, \tau) e^{-\eta/T_1} \exp\{i[(\mathbf{k}_1 + \mathbf{k}_2 - \mathbf{k}_3) \cdot \mathbf{z} - \omega t]\} \\
&\quad \times \frac{1}{T_1} \int_{-\infty}^{\eta} [|E_{10}|^2 + |E_{30}|^2] \mathcal{F}^4(\eta' - 2z/\vartheta_g, \tau) e^{\eta'/T_1} d\eta'.
\end{aligned} \tag{13}$$

From Eqs. (12) and (13) with the boundary condition $\mathcal{E}_4(l, t) = 0$, we obtain the amplitude of the signal field

$$\begin{aligned}
\mathcal{E}_4(0, t, T_d) &= i \frac{2\pi\omega^2}{kc^2} 2\chi^{(3)} E_{10} E_{20} E_{30}^* \mathcal{F}(t - T_d, \tau) \int_0^l \mathcal{F}^2(t - 2z/\vartheta_g, \tau) dz + i \frac{2\pi\omega^2}{kc^2} 2\chi_g^{(3)} E_{10} E_{20} E_{30}^* \\
&\quad \times [|E_{10}|^2 + |E_{30}|^2] \mathcal{F}(t - T_d, \tau) e^{-t/T_1} \frac{1}{T_1} \int_0^l \int_{-\infty}^t \mathcal{F}^4(\eta' - 2z/\vartheta_g, \tau) e^{\eta'/T_1} d\eta' dz,
\end{aligned} \tag{14}$$

where l is the sample length. For a material without two-photon absorption, the DFWM signal will be expressed only by the first term of Eq. (14). In this case, the signal is proportional to the cubic power of the input intensities if all three input beams are derived by splitting one input parent beam. For a material with two-photon absorption, however, the detected DFWM signal involves two contributions, i.e., the coherent DFWM process and the population grating process. The former process is described by the first term in Eq. (14) and the latter process involves the second term in Eq. (14). For zero delay of beam 2, the three incident beam pulses arrive together in the sample cell and the DFWM signal is derived from both the coherent four-wave mixing process and the population grating process. The DFWM signal has a power dependence of between a third order and a fifth order, depending on the relative contributions from the coherent four-wave mixing and the population grating. On the other hand, when beam 2 is delayed beyond the pulse width of the grating forming pulses, the instantaneous coherent four-wave mixing process does not occur, but the population grating contribution is still present if the excited state produced by two-photon absorption has a long enough lifetime. As can be seen from Eq. (14), the DFWM signal, in this case, should obey a fifth-order power dependence on the input intensity.

There is an additional complication which must be considered in order to form a fuller picture of the two-photon-induced DFWM process. The susceptibilities entering equations for the polarization are complex, i.e., they involve both the real part and the imaginary part. The imaginary part of the ground state linear susceptibility $\chi_{a, \text{im}}^{(1)}$ can be taken equal to zero because we assume no one-photon absorption at the frequency ω . Both nonlinear components, i.e., the true third-order susceptibility and the effective nonlinear contribution from excited species, will contain imaginary parts. For $\chi_g^{(3)}$, the presence of the imaginary part derived from $\chi_b^{(1)}$ makes it complex and it simply means that the two-photon-induced species may absorb at ω . The imaginary part of $\chi^{(3)}$ has another simple interpretation. Inserting $\chi^{(3)} = \chi_r^{(3)} + i\chi_{\text{im}}^{(3)}$ in the coupling equation [e.g., Eq. (11)], we verify that the imaginary part of $\chi^{(3)}$ is responsible for nonlinear (two-photon) absorption since it gives rise to a change of the electric field amplitude. Its role is dual. Considering various polarization terms involving $\chi_{\text{im}}^{(3)}$, one notices that since $\mathcal{E}_4 \ll \mathcal{E}_2$

$\ll \mathcal{E}_1 \cong \mathcal{E}_3$, there is no need to consider a two-photon absorption correction in Eq. (12), i.e., cubic terms involving \mathcal{E}_4 can be neglected. However, the cubic term involving $\chi_{\text{im}}^{(3)}$ and $\mathcal{E}_1 \mathcal{E}_2 \mathcal{E}_3^*$ will be important. In Eq. (13), it will produce an amplitude grating and together with the appropriate imaginary term corresponding to the population grating, the cubic term will contribute to the DFWM signal. It should be noted here that the amplitude grating signal is 90° out of phase with the phase grating signal. The total DFWM intensity can be expressed as the sum of squares of these two contributions.

Therefore, a two-photon resonance has the following role: Its presence enhances the real part of $\chi^{(3)}$ and therefore the instantaneous formation of the phase grating, at the same time giving rise to an amplitude grating through the imaginary part of $\chi^{(3)}$. The excited species formed by two-photon absorption contributes to the delayed grating through the induced change in the first-order susceptibility $\chi_b^{(1)} - \chi_a^{(1)}$.

While the two-photon absorption should not be very important for attenuation of beam 4, there may be situations when the attenuation of the strong beams becomes nonnegligible. When the probe beam is much weaker than the two forward pump beams, as with our experiment, one can introduce the first-order correction by simply considering only the attenuation effect on beams 1 and 3. For the sake of simplification, we only consider the change of the peak amplitude of pulse with spatial position z in the medium, i.e., we ignore the change of two-photon absorption with time at a fixed position. We also assume that beams 1 and 3 conform to the same attenuation law. Based on the above assumptions, a spatial attenuation factor $A(z)$ is introduced into Eq. (4). At the same time, the factor $\mathcal{F}(t - z/\vartheta_g, \tau)$ in Eq. (9) is taken as 1. Therefore Eq. (9) becomes

$$\mathcal{E}_j(z) = A(z) E_{j0}, \quad j = 1, 3, \tag{15}$$

where E_{j0} is the peak amplitude of the j th beam at the boundary $z = 0$. By substituting Eq. (15) into the coupling wave equation

$$\frac{\partial \mathcal{E}_1(z)}{\partial z} = -\frac{2\pi\omega^2}{kc^2} \chi_{\text{im}}^{(3)} (\mathcal{E}_1 \mathcal{E}_1^* \mathcal{E}_3 + 2\mathcal{E}_3 \mathcal{E}_3^* \mathcal{E}_1), \tag{16}$$

and assuming that the initial field amplitudes of both pump beams are the same, $E_{10} = E_{30}$, we have

$$\frac{\partial A(z)}{\partial z} = -\frac{2\pi\omega^2}{kc^2} 3\chi_{\text{im}}^{(3)} |E_{10}|^2 A(z)^3. \quad (17)$$

Solving Eq. (17) and using the boundary condition $A(0) = 1$, $A(z)$ is obtained as

$$A(z) = \frac{1}{(1 + 6\mathcal{K}'\chi_{\text{im}}^{(3)} |E_{10}|^2 z)^{1/2}}, \quad (18)$$

where $\mathcal{K}' = 2\pi\omega^2/(kc^2)$ and the peak amplitudes of the fields are taken as

$$\mathcal{E}_j(z) = \frac{E_{j0}}{(1 + 6\mathcal{K}'\chi_{\text{im}}^{(3)} |E_{10}|^2 z)^{1/2}}, \quad j = 1, 3. \quad (19)$$

Combining Eqs. (12), (13), and (19) with the boundary condition $\mathcal{E}_4(l, t) = 0$, we have the peak amplitude of the signal field with the following form under the conditions of $T_d = 0$ and $\mathcal{F}(\eta, \tau) = 1$:

$$\mathcal{E}_{4\text{max}}(z) = i\mathcal{K}'\chi^{(3)} E_{10} E_{20} E_{30}^* \times \frac{\ln[(1 + \beta l)/(1 + \beta z)]}{\beta}, \quad (20)$$

where

$$\beta = \frac{4\pi\omega^2}{kc^2} 3\chi_{\text{im}}^{(3)} E_{10}^2. \quad (21)$$

β is the spatial attenuation coefficient of beams 1 and 3 due to two-photon absorption. Therefore, by comparing Eq. (20) with the usual expression for a third-order nonlinear process without absorption, we find that the following correction factor F for two-photon absorption should be used:

$$F = \frac{\beta l}{\ln[(1 + \beta l)]}. \quad (22)$$

It should be noted that unlike the correction factor used for one-photon absorption, the correction factor F for two-pho-

ton absorption is a function of the incident power intensity.

The theoretical treatment presented above provides the following conclusions:

(i) the DFWM signal contains a “fast” component due to the coherent $\chi^{(3)}$ term and a “slow” component arising from the population grating;

(ii) the relative contributions of both components to the DFWM intensity depend on light intensity, laser pulse duration, and other experimental conditions;

(iii) power dependence of the DFWM signal is different from the usual cubic dependence, the fifth-order power dependence being derived from the two-photon induced population grating;

(iv) it is necessary to introduce an intensity-dependent absorption correction to the DFWM signal which accounts for depletion of pump beams by two-photon absorption.

III. EXPERIMENT

A. Materials preparation

The didecyloxy ($-\text{OC}_{10}\text{H}_{21}$) substituted *para*-polyphenyl oligomers corresponding to the monomer, the trimer, the pentamer, and the heptamer were synthesized for measurement by DFWM. The monomer 1,4-bis(decyloxy)benzene was synthesized in 84% yield by a procedure similar to that described in the literature for the synthesis of aromatic diethers.²⁸ Trimer ($n = 0$), pentamer ($n = 1$), and heptamer ($n = 2$) were synthesized in yields of 53, 41, and 15%, respectively, by a synthetic scheme developed previously for the synthesis of unsubstituted and phenyl substituted *para*-polyphenyls (Fig. 2).²⁹

Although the trimer, the pentamer, and the heptamer were prepared by one-pot procedures, isolation of the trimer and the heptamer intermediates at each step of synthesis was

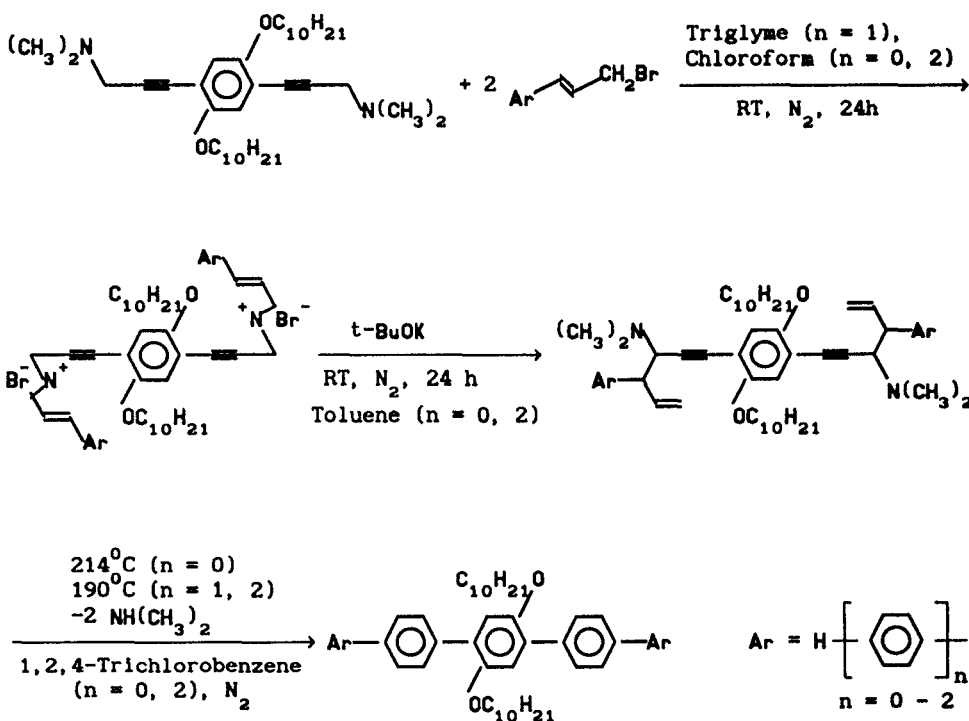


FIG. 2. A synthetic scheme for the preparation of didecyloxy substituted *para*-polyphenyls.

found to increase the overall yield. The advantage of utilizing such a preparatory scheme was the complete isolation of the all *para* isomer from its *ortho-ortho* and *ortho-para* isomers during thermal closure to the final polyphenyls.^{30,31}

The physical characterization of the didecyloxy substituted polyphenyls is summarized in Table I. Typically the yield decreased as the length of the polyphenyl chain increased; this loss of yield was also observed to occur during the preparation of the previously reported polyphenyls utilizing such a route.²⁹ Melting points of the polyphenyls also increased as molecular weight increased. In addition, at higher boiling, more nonpolar solvents were required for recrystallization as the molecular weight of the polyphenyl increased. All polyphenyls studied here were soluble in tetrahydrofuran at room temperature and thus provided a means to prepare dilute solutions of the polyphenyls for DFWM experiments.

B. Measurements

The absorption spectra of the compounds investigated in this study were obtained from their very dilute THF solutions. The spectrometer used in our measurement was Shimadzu UV-260. The cuvette thickness is 1 cm.

The system used in our experimental study of degenerate four-wave mixing is the same as that described in previous publications.^{20,21} It delivers amplified and nearly transform-limited 400 pulses at 602 nm with the repetition frequency of 30 Hz and with the maximum energy of approximately 0.4 mJ per pulse. An appropriate set of beam splitters and mirrors are used to form three beams which can be synchronized using individually adjustable delay lines to be simultaneously incident at the sample. By delaying beam 2 with respect to a pair of forward beams 1 and 3, one can record the temporal profile of the DFWM signal. The signal is monitored with a photodiode and processed with a boxcar averager (EG&G Princeton Applied Research, Model 4200). The data are further processed by a computer.

The intensity of the DFWM signal for the solution is compared to that obtained for a reference sample under

identical conditions. An effective third-order susceptibility for the solution is then calculated from the following equation:

$$\chi^{(3)} = \left(\frac{n}{n_s}\right)^2 \cdot \left(\frac{I}{I_s}\right)^{1/2} \cdot \frac{l_s}{l} \cdot \chi_s^{(3)} \cdot F, \quad (23)$$

where I stands for the DFWM signal intensity, n is the refractive index of the medium, l is the interaction length, and subscript s refers to a reference sample. F is the correction factor taking into account the sample absorption. As there is no one-photon absorption present for the entire family of the compounds investigated here, it appeared necessary to use only the two-photon absorption correction derived in the previous section for the heptamer solution for which the two-photon absorption is strong. For solution measurement, the effective $\chi^{(3)}$ calculated from the above equation contains a contribution from both the solute and the solvent. Therefore, we treat the third-order susceptibility for the solution as the sum of two contributions

$$\chi^{(3)} = \mathcal{L}^4 (N_s \gamma_s + N_x \gamma_x), \quad (24)$$

where γ_s and γ_x stand for the hyperpolarizabilities of the solvent and the solute, respectively. N_s and N_x denote the respective molecular density, i.e., the number of molecules per cubic centimeters, and \mathcal{L} is the local field correction factor approximated by the Lorentz expression¹

$$\mathcal{L} = \frac{n^2 + 2}{3}, \quad (25)$$

where n is the refractive index of a solution at the frequency of the measurement (i.e., 602 nm). The values of n are measured by using an Abbe refractometer at the sodium line (589 nm). No dispersion correction was attempted.

For each compound, the effective $\chi^{(3)}$ value at different concentrations is calculated by using Eq. (23) and the γ values can be obtained by a least-squares fit to Eq. (24). Errors in the determination of γ are calculated taking into account the uncertainties of the measurements of the DFWM intensities for individual points. Other experimental factors, such as the concentration range, the concentra-

TABLE I. Physical characterization of decyloxy substituted polyphenyls.

X mer	Yield (%) ^a	Melting point (°C)	Appearance (solvent)	Solution at 25 °C	Formula (FW)	Elementary analysis calculation (found)	E.I.M.S. <i>m/z</i> (%) ^b
Monomer	84	68° Lit mp 68 ^d	Colorless plates (MeOH)	CHCl ₃ THF	C ₂₆ H ₄₆ O ₂ (390.62)	C, 79.94(79.92) H, 11.87(11.85)	390(25, M ⁺) 110(100)
Trimer (<i>n</i> = 0)	53	65.3–66.3°	White powder (EtOH) ^f	CHCl ₃ THF	C ₃₈ H ₅₄ O ₂ (542.81)	C, 84.08(84.38) H, 10.03(9.86)	542(13, M ⁺) 43(100)
Pentamer (<i>n</i> = 1)	41	123–126°	Yellow needles (2-propanol) ^g	CHCl ₃ Heptane THF	C ₅₀ H ₆₂ O ₂ (694.99)	C, 86.40(86.70) H, 8.98(9.00)	695(19, M ⁺) 43(100)
Heptamer (<i>n</i> = 2)	15	185–187°	Yellow needles (cyclohexane)	THF	C ₆₂ H ₇₀ O ₂ (847.17)	C, 87.89(87.77) H, 8.33(8.35)	847(1, M ⁺) 43(100)

^a Purified yield.

^b Emission ionization mass spectra performed by WRDC/MLSA, Wright–Patterson AFB, OH.

^c Uncorrected.

^d Reference 32.

^e Corrected melting point from Mel-Temp II apparatus with a calibrated Fluke Model 51 thermocouple.

^f After chromatography on a silica gel column using 3:1 chloroform:petroleum ether eluent.

^g After chromatography on a silica gel column using 1:1 methylene chloride:petroleum ether eluent.

tion intervals, the number of solutions, and the laser instability also induce different errors under different conditions.

Equation (24) is supposed to hold for the case when the solution nonlinearity is composed of coherent instantaneous contributions involving real parts of hyperpolarizabilities of the solute and the solvent. In the presence of two-photon absorption, the hyperpolarizability is complex and there is a contribution from the population grating. In this case, we can only treat the derived γ value as an effective quantity and we use the following equation for fitting the concentration dependence:

$$|\chi_{\text{eff}}^{(3)}| = \mathcal{L}^4 [(N_1 \gamma_{1r} + N_2 \gamma_2)^2 + (N_1 \gamma_{1i})^2]^{1/2}, \quad (26)$$

where γ_{1r} and γ_{1i} represent the real and the imaginary parts of the complex second hyperpolarizability of the solute, respectively, and γ_2 is the second hyperpolarizability for THF, for which we assume no imaginary part.

We have also performed studies of the power dependence of the DFWM signal. The intensity of the incident beams is changed with a pair of polarizers. In order to minimize the measurement errors, each data point is averaged for over 30 laser pulses. During these studies, the intensities of the incident beams were chosen so that the saturation of the DFWM signal is avoided.

IV. RESULTS AND DISCUSSION

A. Linear UV-visible absorption

The UV-visible absorption spectra of the alkoxy substituted poly-*p*-phenyls in THF are shown in Fig. 3 where the concentration for each molecule is 2×10^{-5} M. The transitions observed in these systems can be of $n\pi^*$ or $\pi\pi^*$ type. We leave the precise assignment of the transitions to more detailed studies of the energetic levels in substituted polyphenyls and discuss the spectra only in a qualitative manner.

Two absorbance peaks are observed in the monomer. For the trimer, there are three absorption maxima. One can

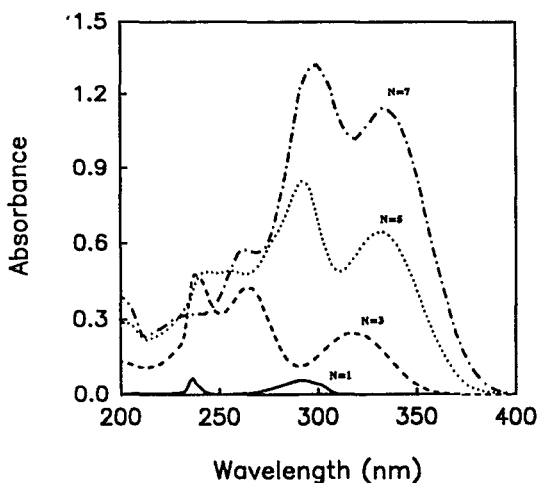


FIG. 3. UV-visible absorption spectra for the monomer and the various oligomers in THF solution. The concentration for each molecule is 2×10^{-5} M and the cell thickness is 1 cm. The numbers 1, 3, 5, and 7 represent the monomer, the trimer, the pentamer, and the heptamer, respectively.

expect that for a quasi-one-dimensional system, there should be several absorption transitions corresponding to the various phase relations between the repeat units. The lowest energy excitation should be that for all units excited in phase. Other transitions will be more or less localized to one or more repeat units. Indeed, the shortest wavelength transition in the trimer has almost the same wavelength as one of the transitions in the monomer, which may imply that it represents the local absorption of one phenyl unit. Two long wavelength peaks in the trimer have their analogs in the pentamer and the heptamer. They show an expected red shift with the elongation of the π -electron system. We notice, however, that the shift between the pentamer and the heptamer is already very small, possibly indicating that long polyphenyl chains exhibit poor overlap of π electrons due to their deviation from planarity.

The positions of the absorption peaks (λ_{max}) and the linear absorption coefficients at each peak are summarized in Table II. Figure 4 shows the dependence of the transition energies for the two low energy transitions on the number of phenyl units. The near leveling off for the π -electron conjugation after the pentamer is clearly seen. The introduction of a long alkoxy chain increases the steric hindrance between the substituted phenyl ring and the neighboring rings; the π -electron overlap for the oligomer is therefore reduced.

B. Second hyperpolarizability

The second hyperpolarizabilities γ for these oligomers are calculated by measuring the DFWM signals in a series of THF solutions. The concentration range used for each oligomer is limited by its maximum solubility. Although the monomer has a reasonably high solubility in THF, its relatively small third-order hyperpolarizability produces a relatively large experimental error during the measurement. For larger oligomers, the reduced solubility is compensated by a much higher third-order nonlinearity and the experimental error in determination of the effective hyperpolarizability is lower.

For the heptamer solutions exposed to our laser beam (602 nm), we observe a very strong visible blue (upconverted) fluorescence even at a concentration as low as 0.001 M. The pentamer shows a much weaker blue fluorescence compared to the heptamer in a comparable concentration range. The monomer and the trimer solutions did not show any visible fluorescence in the experimental concentration range used. Since a blue light emission is observed in solutions of the pentamer and the heptamer, there is strong evidence that a two-photon absorption takes place at 602 nm within the power range used in our measurements. The presence of two-photon-induced excited species is likely to contribute to the DFWM signal by formation of a population grating. The first indication that the two-photon processes are of importance for the pentamer and the heptamer comes from the comparison between the temporal profiles of the DFWM signal for a trimer solution (Fig. 5) and those of a heptamer solution (Fig. 6). For the trimer (as well as for the monomer), we observe a symmetric temporal response, the width of which is most likely limited only by the width of the laser pulses used, together with the geometrical factors (the

TABLE II. The peak absorption wavelength, the respective bandgap, the linear absorbance coefficients, and the third-order hyperpolarizabilities for didecyloxy substituted *p*-polyphenyl oligomers.

	Monomer	Trimer	Pentamer	Heptamer
$\lambda(\text{nm})^a$	291.9	318.9	331.4	335.8
$\nu \times 10^{-4} (\text{cm}^{-1})$	3.426	3.136	3.018	2.978
$\epsilon (\ell \text{mol}^{-1} \text{cm}^{-1})$	2800	12 300	31 900	32 000
$\lambda(\text{nm})^b$	238.2	266.1	289.6	299.6
$\nu \times 10^{-4} (\text{cm}^{-1})$	4.198	3.758	3.453	3.338
$\epsilon (\ell \text{mol}^{-1} \text{cm}^{-1})$	3200	21 000	32 000	42 000
$\gamma(\text{esu})^c$	2.2×10^{-35}	6.9×10^{-35}	3.5×10^{-34}	$-3.3 \times 10^{-33}(\text{r})$ $7.2 \times 10^{-33}(\text{im})$

^aThe peak wavelength refers to the lowest energy transition for the monomer through the heptamer.

^bThe peak wavelength refers to the second lowest energy transition for the monomer through the heptamer.

^cOrientationally averaged scalar part of the third-order hyperpolarizability.

thickness of the sample). In other words, there is no indication of formation of a population grating, i.e., a grating formed by excited species that can live much longer than the pulse width. On the contrary, for the pentamer and the heptamer, the temporal behavior of the DFWM signal is different, indicating a fast response superimposed on a slow decay. We can rule out a contribution of ordinary one-photon absorption to the formation of the slow component in DFWM since our measurement wavelength of 602 nm is far away from the λ_{max} of one-photon absorption (340 nm) of the heptamer.

As discussed in the theoretical section, the decay time of the coherent four-wave mixing process is determined by the pulse width of the laser beam, but the decay time of the population grating process is determined by the lifetime of the molecular excited state. By comparing the temporal behaviors of the DFWM signal for the trimer and the heptamer solutions as shown in Figs. 5 and 6, it can be seen that the four-wave mixing process in the trimer solution is dominated by coherent interaction of the light beams because it shows only a fast component. In the heptamer solution, there seems to be a dominance of the population grating process induced by two-photon absorption as evidenced by the very slow decay of the DFWM signal.

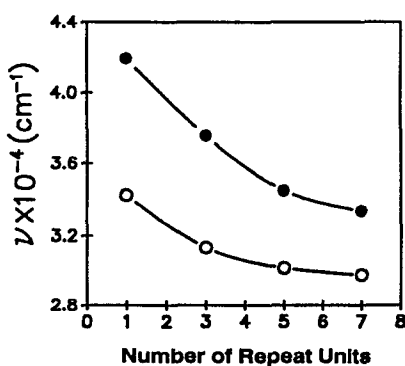


FIG. 4. The bandgap dependence on the number of phenyl units. The curve with open circle data points represents the lowest energy transition and the curve with solid circle data points stands for the second lowest energy transition.

For a quantitative correlation between the theoretical description presented above and the experimentally observed time-resolved DFWM signal obtained for the trimer solution we use Eq. (14), limiting it to the terms which describe the coherent four-wave mixing process only. As shown in Fig. 5, the theoretical fit to the experimental curve is excellent, confirming the assumption that the DFWM signal for the trimer solution is derived from the coherent four-wave mixing process. For the experimental as well as the theoretical curves, a plateau is obtained for the trimer solution. The occurrence of the plateau is due to the fact that the geometric length corresponding to the pulse width of the laser is much shorter than the sample thickness. Since the laser pulse width used in our experiment is about 500 fs, the spatial overlap length for two counterpropagating laser pulses is about 0.15 mm, which is much shorter than the sample thickness of 1 mm. As a result, a full overlap of three laser pulses (yielding the maximum DFWM signal) will occur within the sample cell for a period of time which corresponds to the plateau of the DFWM signal when the backward pump beam is delayed. Therefore, the width of the signal plateau is determined by the sample thickness.

For the DFWM signal obtained for the heptamer solution, both the coherent four-wave mixing and the two-pho-

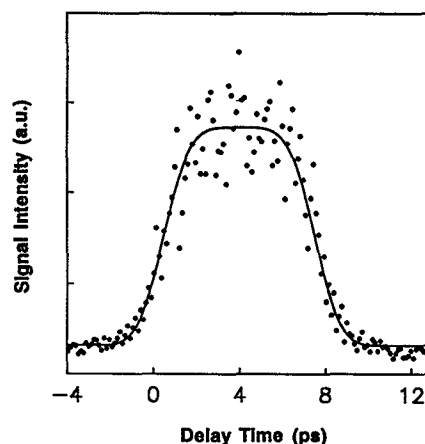


FIG. 5. The temporal DFWM profile for the trimer solution obtained by delaying beam 2. The solid curve is a theoretical fit.

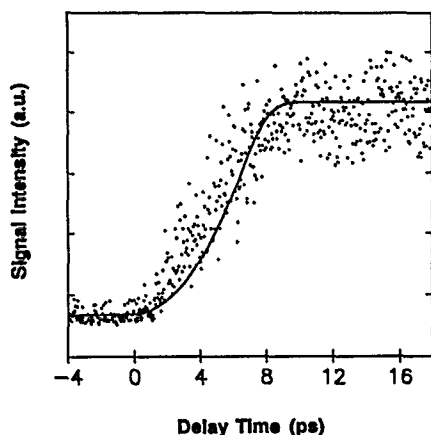


FIG. 6. The temporal DFWM profile for the heptamer solution obtained by delaying beam 2. The solid curve is a theoretical fit.

ton absorption-induced population grating processes are involved. However, it can be seen from our experimental data curve that the DFWM signal for the solution shows a very long decay as shown in Fig. 6, which indicates that it is dominated by the population grating process. For this reason, we use the population grating terms of Eq. (14) to correlate theory with the experimental results. The solid curve in Fig. 6 shows the theoretical fit. The slight deviation of the theoretical curve from the experimental data points in the rising part of the signal may be due to the neglect of the contribution of the coherent four-wave mixing process in our theoretical fit.

The contribution of two-photon absorption of the heptamer to its overall behavior in the third-order nonlinear optical processes is also reflected in the concentration dependence of the measured $\chi^{(3)}$ value. In the concentration dependence curve shown in Fig. 7, a dip is found at low concentrations. The presence of such a dip can be explained by assuming that the real part $\chi^{(3)}$ of the solute has a sign opposite to that of the solvent.^{1,33} However, if only the real parts of $\chi^{(3)}$ for both the solvent and the solute contribute, the DFWM signal for the solution will disappear completely at a

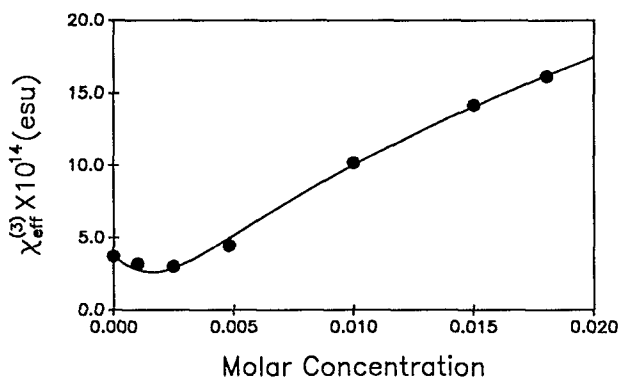


FIG. 7. The concentration dependence of $\chi^{(3)}$ for the heptamer solution. The dip at low concentration implies that the real part of γ or $\chi^{(3)}$ for the heptamer has an opposite sign to that of THF.

certain concentration. This is not observed in our measurements. Therefore, we assume that the second hyperpolarizability γ for the heptamer is a complex quantity at 602 nm. In terms of the transient grating description of the DFWM process, a complex $\chi^{(3)}$ means that there are contributions from both the phase (refractive index) and the amplitude (absorption coefficient) gratings. These contributions are 90° out of phase with each other and, therefore, the DFWM signal is proportional to the sum of their squares. Accordingly, we have fitted the concentration dependence of the effective $\chi^{(3)}$ value for the heptamer solutions using Eq. (26).

It was necessary to adopt a slight absorption correction in order to obtain a good fit of the concentration dependence at the concentrations investigated. The absorption correction, which was found from the fit using Eq. (22), gives a spatial attenuation coefficient equal to 7.34 cm^{-1} . This coefficient corresponds to an estimated peak light intensity of $I = 10 \text{ GW/cm}^2$. This value of β is therefore equivalent to a two-photon absorption cross section $\kappa_2 = 4.2 \times 10^{-25} \text{ cm}^4 \text{ s/erg}^2$. Furthermore,

$$\gamma_{\text{im}} = \frac{\kappa_2 h n^2 c^2}{32 \pi^3 \mathcal{L}^4} \quad (27)$$

where \mathcal{L} is the local field factor and h is the Planck constant. γ_{im} obtained from Eq. (27) is $1.5 \times 10^{-32} \text{ esu}$, a value that is in reasonable agreement with the one obtained using the concentration dependence analysis involving Eq. (26). One should note here that this agreement is remarkably good, since the fit of the concentration dependence relies on the comparison of the DFWM signal for the solution to that of the solvent, from which both the real and the imaginary parts of γ are obtained. The determination of γ_{im} by estimation of the spatial attenuation coefficient is, on the other hand, an absolute way of measuring the imaginary component of the hyperpolarizability and, therefore, is heavily dependent on the simplifying assumptions about the laser pulse geometric and temporal shapes as well as on additional complications due to, e.g., self-focusing (actually, in the case of the heptamer solutions, we should expect a self-defocusing effect, because of the real part of γ being negative).

Table II lists the effective γ values obtained from our measurements. These values increase from the monomer to the trimer, with a more rapid increase from the trimer to the pentamer and to the heptamer. The dependence of γ on the number of repeat units is shown in Fig. 8. The increase of γ from the monomer to the trimer can be expected from the conjugation length change between the two oligomers. However, the rapid γ increase from the trimer to the pentamer and especially to the heptamer is clearly not only the result of conjugation elongation, but is due to the two-photon resonant behavior. In the cases of the monomer and the trimer, the hyperpolarizability seems to contain only a real part. In the case of the pentamer, there is an indication of the presence of the imaginary part, although we have not been able to obtain a good fit which would allow us to separate these parts. In the case of the heptamer, however, the imaginary part of γ dominates the complex hyperpolarizability. This is an effective value, which apart from the instantaneous part contains a contribution from the population grating effects.

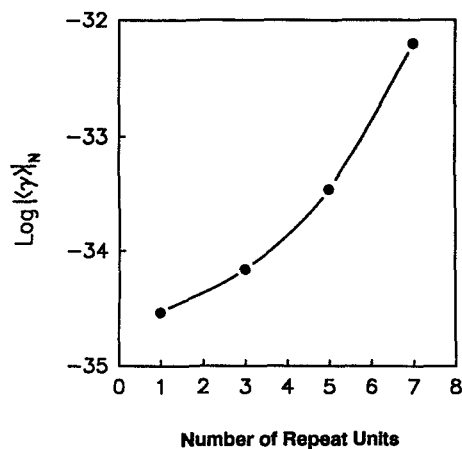


FIG. 8. The dependence of γ values on the number of repeat phenyl units.

C. Power dependence

For a nonresonant degenerate four-wave mixing process, the intensity of the DFWM signal can be written as follows:

$$I_4(\omega, t) = [\omega / (2\epsilon_0 c n_0^2)]^2 (\chi^{(3)})^2 I_1(\omega, t) I_2(\omega, t) \times I_3(\omega, t), \quad (28)$$

where I_4 is the DFWM signal intensity. I_1 , I_2 , and I_3 are the intensities of counterpropagating radiation fields $E_1(\omega, t)$, $E_2(\omega, t)$, and $E_3(\omega, t)$, respectively. The term l is the interaction length. Therefore, if the ratios of intensities of the three incident beams are kept constant, and they are derived from the same source, a cubic dependence of the DFWM signal on the source intensity should be observed. For solutions of the monomer and the trimer, we have in fact established this power dependence. In the case of contribution from a one-photon resonance, a population grating can be formed. However, in the absence of any saturation of absorption, a cubic dependence of DFWM on the source intensity should still be observed.

When a two-photon absorption is dominant, one can expect the appearance of a different power dependence. Therefore, we have performed the power dependence studies for various delays of the backward beam, i.e., within different regions of the DFWM signal temporal profile for solutions of both the pentamer and the heptamer. At the delay times of the backward probe beam corresponding to the rising edge of the DFWM signal temporal profile, the slopes of the output–input intensity dependence in a log–log plot are about 4 and 4.5 for the pentamer and the heptamer solutions, respectively. For the delay corresponding to the maximum of the DFWM signal temporal profile, the slopes for both the pentamer and the heptamer solutions are close to 5. As an example, Fig. 9 shows the power dependences for the heptamer solution (0.02 M) at different regions of the DFWM signal temporal profile. These experimental results can be well interpreted by referring to the theoretical predictions of Sec. II. There seems to be a smaller contribution from a two-photon absorption induced population grating for the pentamer solution than for the heptamer solution. The relative

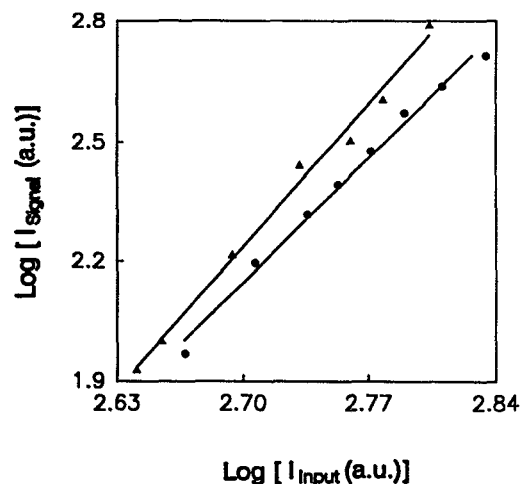


FIG. 9. The power dependence for the heptamer solution: filled triangles refer to a situation of pure population grating process; filled circles represent a situation when both the coherent four-wave mixing process and the populating grating contribution coexist (delay time is 4 ps as shown in Fig. 6).

importance of the coherent DFWM and the population grating terms depends, however, on the delay time. At the maximum of the DFWM signals, the two-photon population grating terms are dominant for both the pentamer and the heptamer. Once more, these experimental results confirm that the high values of the effective third-order nonlinear parameters for the pentamer and the heptamer are due to two-photon absorption.

V. CONCLUSIONS

We have investigated the third-order optical nonlinearities for a series of sequentially built poly-*p*-phenyl oligomers. The following conclusions can be drawn from the experimental studies:

(i) For the substituted poly-*p*-phenyl oligomers, their effective third-order nonlinearity increases with the number of repeat phenyl units. The γ increase from the monomer to the trimer can be expected on the basis of the π -conjugation elongation. The π -conjugation length (represented by the position of the absorption maximum) does not increase very rapidly from the trimer to the pentamer to the heptamer. However, a rapid increase for the effective γ value is observed from the trimer to the pentamer to the heptamer. This increased effective γ value has contributions from both the coherent four-wave mixing process and the two-photon absorption-induced population grating process.

(ii) The γ value for a two-photon absorbing material calculated using the conventional DFWM theory is not the true nonresonant γ value. The calculated γ value is an effective value which is actually a function of the intensity, sample thickness, and the laser pulse width. Therefore, the measured γ values for the pentamer and the heptamer can only be treated as effective values.

(iii) The power dependence study of the DFWM signal shows that a nonlinear material with two-photon absorption exhibits different power dependence laws in different regions

of the DFWM temporal profile. A fifth-order power dependence is observed in the time regime where pure population grating effects are dominant. A power dependence between third order and fifth order is observed in the time regime where both the coherent four-wave mixing and the two-photon-induced population grating contribute.

(iv) The presence of a two-photon resonance manifests itself in the increase of the effective nonlinearity, which in the case of DFWM involves both the real and the imaginary parts of $\chi^{(3)}$. However, two-photon absorption also leads to the depletion of the pump beams. This depletion can be accounted for by using the expression derived in the theoretical section.

ACKNOWLEDGMENTS

The work performed at SUNY, Buffalo was supported by the Air Force Office of Scientific Research, Directorate of Chemical and Atmospheric Sciences and Polymer Branch, Air Force Wright Materials Laboratory, Wright Research and Development Center through Contract No. F49620-90-C-0021.

¹P. N. Prasad and D. J. Williams, *Introduction to Nonlinear Optical Effects in Molecules and Polymers* (Wiley, New York, 1991).

²*Nonlinear Optical and Electroactive Polymers*, edited by P. N. Prasad and D. R. Ulrich (Plenum, New York, 1989).

³J. Zyss, *J. Mol. Electron.* **1**, 15 (1985).

⁴D. J. Williams, *Angew. Chem. Int. Ed. Engl.* **23**, 690 (1984).

⁵C. Maloney and W. Blau, *J. Opt. Soc. Am. B* **14**, 1035 (1987).

⁶D. Sarid and G. I. Stegeman, *J. Appl. Phys.* **52**, 5439 (1981).

⁷C. Liao and G. I. Stegeman, *Appl. Phys. Lett.* **44**, 164 (1984).

⁸R. Reinisch and G. Vitrant, *J. Appl. Phys.* **67**, 6671 (1990).

⁹R. W. Hellwarth, D. M. Pennington, and M. A. Hennesian, *Phys. Rev. A* **41**, 2766 (1990).

¹⁰M. Segev, Y. Ophir, and B. Fischer, *Appl. Phys. Lett.* **56**, 1086 (1990).

¹¹N. C. Kothari and S. C. Abbi, *Prog. Theor. Phys.* **83**, 414 (1990).

¹²M. J. Soileau, W. E. Williams, N. Mansour, and E. W. Van Stryland, *Opt. Eng.* **28**, 1133 (1989).

¹³T. Morioka and M. Saruwatari, *Opt. Eng.* **29**, 200 (1990).

¹⁴Y. Silberberg and B. G. Sfez, *J. Phys. Colloq. C2*, 283 (1988).

¹⁵B. Van Wonterghem, S. M. Saltiel, and P. M. Rentzepis, *J. Opt. Soc. Am. B* **6**, 1823 (1989).

¹⁶C. Denz, J. Goltz, and T. Tschudi, *Opt. Commun.* **72**, 129 (1989).

¹⁷D. M. Pepper, *Phys. Rev. Lett.* **62**, 2945 (1989).

¹⁸S. Mailhot, P. Galarneau, R. A. Lessard, and M. M. Denariez-Roberge, *Appl. Opt.* **27**, 3418 (1988).

¹⁹C. Pare, M. Piche, and P. A. Belanger, *J. Opt. Soc. Am. B* **5**, 679 (1988).

²⁰M. T. Zhao, B. P. Singh, and P. N. Prasad, *J. Chem. Phys.* **89**, 5535 (1988).

²¹M. T. Zhao, M. Samoc, B. P. Singh, and P. N. Prasad, *J. Phys. Chem.* **93**, 7916 (1989).

²²X. F. Cao, J. P. Jiang, D. P. Bloch, R. W. Hellwarth, L. P. Yu, and L. Dalton, *J. Appl. Phys.* **65**, 5012 (1989).

²³R. A. Fisher, *Optical Phase Conjugation* (Academic, New York, 1983).

²⁴H. Eichler, P. Gunther, and D. W. Pohl, *Laser Induced Dynamic Grating* (Springer, Berlin, 1986).

²⁵Y. P. Cui, M. T. Zhao, G. S. He, and P. N. Prasad, *J. Phys. Chem.* (in press).

²⁶M. Samoc and P. N. Prasad, *J. Chem. Phys.* **91**, 6643 (1989).

²⁷Y. R. Shen, *The Principles of Nonlinear Optics* (Wiley, New York, 1984).

²⁸F. Fages, J. P. Desuergne, and H. Bouas-Laurent, *Bull. Soc. Chim. France* **5**, 959 (1985).

²⁹M. R. Unroe and B. A. Reinhardt, *Synthesis* **11**, 981 (1987).

³⁰T. Jemisonm, T. Laird, W. D. Ollis, and I. O. Sutherland, *J. Chem. Soc. Perkin Trans. 1*, 1436 (1980).

³¹T. Laird, W. D. Ollis, and I. O. Sutherland, *J. Chem. Soc. Perkin Trans. 1*, 1473 (1980).

³²J. H. Wernitz, U.S. Patent 2,067,960, Jan. 1937.

³³M. L. Shand and R. R. Chance, *ACS Symp. Ser.* **233**, 187 (1983).